

Reactions of the cationic complex $[(\eta^6\text{-C}_6\text{Me}_6)_2\text{Ru}_2(\mu_2\text{-H})_3]^+$ with nitrogen-containing heterocycles in aqueous solution

Manfred Jahncke, Antonia Neels, Helen Stoeckli-Evans, Georg Süss-Fink *

Institut de Chimie, Université de Neuchâtel, Avenue de Bellevaux 51, CH-2000 Neuchâtel, Switzerland

Abstract

The dinuclear cation $[(\eta^6\text{-C}_6\text{Me}_6)_2\text{Ru}_2(\mu_2\text{-H})_3]^+$ (**1**) reacts in aqueous solution with pyrazole and 4-methylpyrazole to give the bipyrazolato complexes $[(\eta^6\text{-C}_6\text{Me}_6)_2\text{Ru}_2(\mu_2\text{-H})(\mu_2\text{-}\eta^1, \eta^1\text{-N}_2\text{C}_3\text{H}_2\text{R})_2]^+$ (R = H: **2**, R = Me: **3**). The reaction with 1,2,4-triazole results in the formation of the bistriazolato complex $[(\eta^6\text{-C}_6\text{Me}_6)_2\text{Ru}_2(\mu_2\text{-H})(\mu_2\text{-}\eta^1, \eta^1\text{-N}_3\text{C}_2\text{H}_2)_2]^+$ (**4**). Successive protonation of the triazolato ligands in **4** leads to the complexes $[(\eta^6\text{-C}_6\text{Me}_6)_2\text{Ru}_2(\mu_2\text{-H})(\mu_2\text{-}\eta^1, \eta^1\text{-N}_3\text{C}_2\text{H}_2)(\mu_2\text{-}\eta^1, \eta^1\text{-N}_3\text{C}_2\text{H}_3)]^{2+}$ (**5**) and $[(\eta^6\text{-C}_6\text{Me}_6)_2\text{Ru}_2(\mu_2\text{-H})(\mu_2\text{-}\eta^1, \eta^1\text{-N}_3\text{C}_2\text{H}_3)_2]^{3+}$ (**6**). The reaction of **1** with 1,2,3-triazole gives a 1:1 mixture of the bistriazolato complexes $[(\eta^6\text{-C}_6\text{Me}_6)_2\text{Ru}_2(\mu_2\text{-H})(\mu_2\text{-}\eta^1, \eta^1\text{-N}_3\text{C}_2\text{H}_2)_2]^+$ with parallel (**7a**) and anti-parallel (**7b**) coordination of the triazolato ligands. The single-crystal X-ray structure analyses of **2** (hexafluorophosphate salt) and **4** (tosylate salt) reveal for both complex types a ruthenium–ruthenium backbone being bridged by the two heterocyclic ligands with the N–N axis coordinated in a $\mu_2\text{-}\eta^1, \eta^1$ -fashion. A single-crystal X-ray structure analysis of title complex **1** (hexafluorophosphate salt) confirms the presence of three bridging hydrido ligands with a Ru–Ru distance of only 2.47 Å. © 1998 Elsevier Science S.A. All rights reserved.

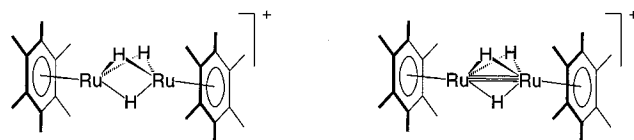
Keywords: Aqueous solution; Hexamethylbenzene complexes; Hydrido ligands; Pyrazolato ligands; Ruthenium; Triazolato ligands

1. Introduction

The chemistry of water-soluble organometallic complexes is a relatively new area of research which is receiving a steadily growing interest [1–8]. Recently we reported on the preparation of the dinuclear cation $[(\eta^6\text{-C}_6\text{Me}_6)_2\text{Ru}_2(\mu_2\text{-H})_3]^+$ (**1**) in aqueous solution and its reactivity towards borohydride reagents [9] as well as towards hydrazine [10]. Complex **1**, first synthesized by M.A. Bennett et al. in organic media [11,12], is a very interesting species for reactions in aqueous solution, since it is water-soluble, stable to hydrolysis, and electron-deficient. The electron-deficiency of **1** can be expressed either by formulating three 3c–2e bonds or, more conventionally, by formulating a ruthenium–ruthenium triple bond being bridged by three hydrido ligands. For the sake of systematics and predictability on the basis of the 18e rule, we have chosen the latter representation (Scheme 1).

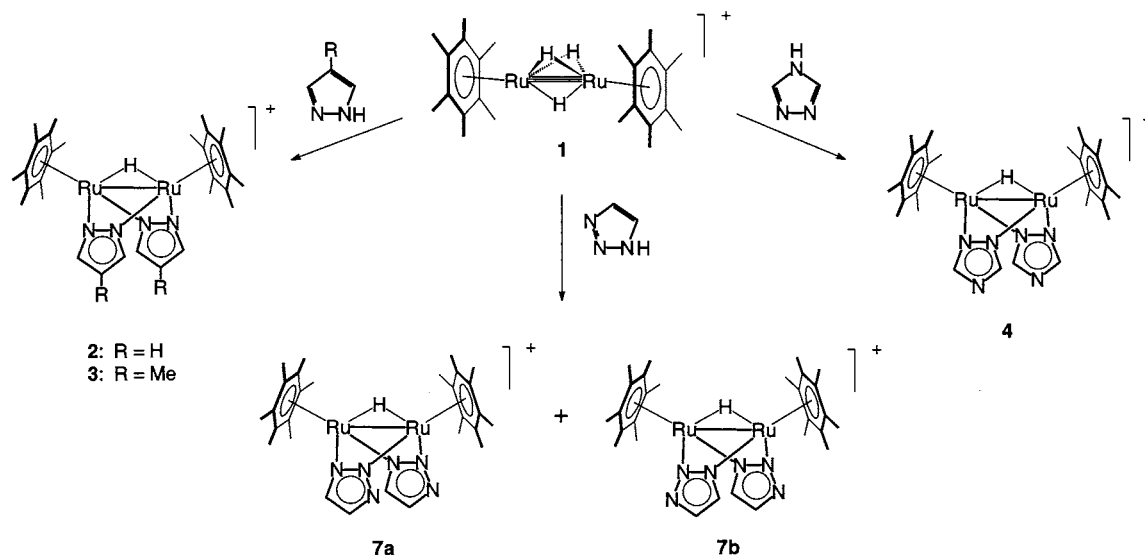
Due to its electron-deficiency, **1** is susceptible to nucleophilic attack. In our systematic study of its reactivity in aqueous solution, we have now investigated the reactions of **1** with nitrogen-containing heterocycles comprising a N–N backbone, such as pyrazole and the triazoles. Both, pyrazole and 1,2,4-triazole, are known to coordinate to metal centers either intact as neutral molecules or deprotonated as anionic ligands.

For pyrazole, mono- and bidentate coordination at one metal center as well as bridging of two metal centers have been observed [13]. The bidentate coordination of a pyrazolato ligand to one metal center is only reported for complexes of the f-block metals, e.g.



Scheme 1. Two possible representations of the cation $[(\eta^6\text{-C}_6\text{Me}_6)_2\text{Ru}_2(\mu_2\text{-H})_3]^+$ (**1**).

* Corresponding author. Tel.: +41 32 7182405; fax: +44 32 7182511; e-mail: georg.suess-fink@ich.unine.ch

Scheme 2. Synthetic routes to complexes **2**, **3**, **4**, **7a**, and **7b**.

in $[(\eta^5\text{-C}_5\text{Me}_5)_2\text{U}(\eta^2\text{-N}_2\text{C}_3\text{H}_3)_2]$ [14]. An example for an arene–ruthenium complex containing the pyrazole ligand in the monodentate coordination mode is $[(\eta^6\text{-C}_6\text{H}_6)\text{RuCl}(\text{HN}_2\text{C}_3\text{H}_3)_2]^+$ [15], whereas the neutral complex $[(\eta^6\text{-C}_6\text{H}_4\text{MePr}^i\text{-}p)\text{RuCl}(\text{HN}_2\text{C}_3\text{H}_3)(\text{N}_2\text{C}_3\text{H}_3)_2]$ contains the monodentate pyrazole ligand as well as two monodentate pyrazolato ligands [16]. The most frequently encountered bridging coordination mode of the pyrazolato ligand is found in the arene–ruthenium complexes $[(\eta^6\text{-C}_6\text{H}_6)_2\text{Ru}_2(\mu_2\text{-Cl})(\mu_2\text{-}\eta^1, \eta^1\text{-N}_2\text{C}_3\text{H}_3)]^+$, $[(\eta^6\text{-C}_6\text{H}_6)_2\text{Ru}_2(\mu_2\text{-Cl})(\mu_2\text{-}\eta^1, \eta^1\text{-N}_2\text{C}_3\text{H}_3)_2]^+$ [15], $[(\eta^6\text{-arene})_2\text{Ru}_2(\mu_2\text{-OH})(\mu_2\text{-}\eta^1, \eta^1\text{-N}_2\text{C}_3\text{H}_3)_2]^+$, and $[(\eta^6\text{-arene})_2\text{Ru}_2(\mu_2\text{-OMe})(\mu_2\text{-}\eta^1, \eta^1\text{-N}_2\text{C}_3\text{H}_3)]^+$ (arene = $\text{C}_6\text{-H}_4\text{MePr}^i\text{-}p$, C_6Me_6) [17,18].

For 1,2,4-triazole, the $\mu_2\text{-}\eta^1, \eta^1$ -bridging coordination mode is also the most frequently encountered, with the neutral triazole as well as with the deprotonated triazolato ligand [19–22]. In the polymer complex $[\text{Fe}(\text{HN}_3\text{C}_2\text{H}_2)_2(\text{N}_3\text{C}_2\text{H}_2)]_n^+$ both the neutral triazole ligand and the anionic triazolato ligand are present, the heterocyclic ligands using two nitrogen atoms for coordination to give rise to a linear chain structure [19]. When all three nitrogen atoms of the triazolato ligand are used for coordination, a layered structure such as in $[\text{Zn}(\text{N}_3\text{C}_2\text{H}_2)\text{Cl}]_n$ may result [23].

2. Results and discussion

2.1. Reaction of $[(\eta^6\text{-C}_6\text{Me}_6)_2\text{Ru}_2(\mu_2\text{-H})_3]^+$ (**1**) with pyrazole and its methyl derivatives

The reaction of an aqueous solution of $[(\eta^6\text{-C}_6\text{Me}_6)_2\text{Ru}_2(\mu_2\text{-H})_3]^+$ (**1**) with pyrazole gives rise to the dipyrazolato complex $[(\eta^6\text{-C}_6\text{Me}_6)_2\text{Ru}_2(\mu_2\text{-H})(\mu_2\text{-}\eta^1, \eta^1\text{-N}_2\text{C}_3\text{H}_3)_2]^+$ (**2**) (Scheme 2). Complex **2** is observed as the only product; even when the reaction is incomplete, no monosubstituted pyrazolato-complex can be detected by ^1H NMR spectroscopy. Cation **2** can be easily isolated from the aqueous solution by precipitation as the hexafluorophosphate salt.

The reaction requires either heating (100°C) or acidification of the solution to pH 3. In the first case the reaction is complete within 2 h, whereas in the latter case completion takes 2 days. The starting complex **1** formally releases two hydride anions in the course of the reaction, which presumably form dihydrogen with the protons present in the solution, a process which should be activated by acid.

Complex **2** is characterized by ^1H NMR, mass spectrometry, microanalysis and a single-crystal X-ray structure analysis. The ^1H NMR spectra exhibit the presence of two pyrazolato and one hydrido ligand per dinuclear (C_6Me_6) $_2\text{Ru}_2$ unit (Table 1). The FAB mass spectrum contains an envelope of peaks centered at m/z 663 which is in agreement with the isotopic distribution of cation **2**.

Complex **2** is characterized by ^1H NMR, mass spectrometry, microanalysis and a single-crystal X-ray structure analysis. The ^1H NMR spectra exhibit the presence of two pyrazolato and one hydrido ligand per dinuclear (C_6Me_6) $_2\text{Ru}_2$ unit (Table 1). The FAB mass spectrum contains an envelope of peaks centered at m/z 663 which is in agreement with the isotopic distribution of cation **2**.

The reactions of **1** with the methyl-substituted derivatives of pyrazole have also been tested in aqueous solution. With 4-methylpyrazole the reaction proceeds in an analogous fashion as with unsubstituted pyrazole; only the disubstituted product $[(\eta^6\text{-C}_6\text{Me}_6)_2\text{Ru}_2(\mu_2\text{-H})(\mu_2\text{-}\eta^1, \eta^1\text{-N}_2\text{C}_3\text{H}_2\text{CH}_3)_2]^+$ (**3**) is formed (Scheme 2). Complex **3** can be isolated from the aqueous solution by precipitation as the hexafluorophosphate salt. The molecular constitution of **3** has been ascertained by ^1H NMR (Table 1), ^{13}C NMR, electrospray mass spectrometry, and microanalysis.

The reaction of **1** with 3-methyl- and with 3,5-dimethylpyrazole, on the other hand, does not lead to

Table 1
 ^1H NMR data of complexes 1–7

Complex	Anion	Solvent	C_6Me_6 (all s, 36H)	Hydrido ligands	N-ligands
1	SO_4^{2-}	D_2O	2.27	–16.41 (3H)	—
1	PF_6^-	CD_3COCD_3	2.38	–15.91 (3H)	—
2	SO_4^{2-}	D_2O	2.25	–15.64 (1H)	7.44 (d, $J=2.0$ Hz, 2H, H-3 and H-5); 6.00 (t, $J=2.0$ Hz, 1H, H-4)
2	PF_6^-	CD_3COCD_3	2.38	–15.71 (1H)	7.38 (d, $J=2.2$ Hz, 1H, H-3 and H-5); 5.92 (t, $J=2.2$ Hz, 2H, H-4)
3	SO_4^{2-}	D_2O	2.23	–15.73 (1H)	2.09 (s, 3H, CH_3), 7.20 (s, 2H, H-3 and H-5)
3	PF_6^-	CD_3COCD_3	2.36	–15.83 (1H)	1.92 (s, 3H, CH_3), 7.19 (s, 2H, H-3 and H-5)
4	SO_4^{2-}	D_2O	2.26	–15.65 (1H)	8.00 (s, 4H)
4	PF_6^-	CD_3COCD_3	2.44	–15.66 (1H)	7.96 (s, 4H)
5	SO_4^{2-}	D_2O	2.31	–15.53 (1H)	8.53 (s, 4H)
5	PF_6^-	CD_3COCD_3	2.49	–15.50 (1H)	at 21°C: 8.55 (s, 4H) at –90°C: 8.2 (br, 2H, $\text{C}_2\text{H}_2\text{N}_3$), 9.3 (br, 2H, $\text{HC}_2\text{H}_2\text{N}_3$)
6	PF_6^-	CD_3COCD_3	2.54	–15.43 (1H)	9.14 (s, 4H)
7 ^a	SO_4^{2-}	D_2O	2.28/2.29 (7a)	–15.37 and –15.38 (each 1H) ^b	— ^c
7 ^a	PF_6^-	CD_3COCD_3	2.285 (7b) 2.41/2.42 (7a) 2.415 (7b)	–15.44 and –15.46 (each 1H) ^b	7.45 (d, 0.8 Hz, 1H) and 7.46 (d, 0.8 Hz, 1H) ^b 7.72 (d, 0.8 Hz, 1 H) and 7.73 (d, 0.8 Hz, 1H) ^b

^a Integration shows that 7a and 7b are formed in a 1:1 ratio.

^b Assignment of the pairs of signals to 7a and 7b not possible.

^c No signal attributable to the coordinated ligand due to the presence of different forms of the free ligand in the reaction mixture.

the analogous products. Instead, slow degradation of **1** being due to the acidic medium is observed by ^1H NMR spectroscopy, giving rise to the formation of the known [24] mononuclear triaqua-complex $[(\eta^6\text{-C}_6\text{Me}_6)\text{Ru}(\text{H}_2\text{O})_3]^{2+}$. This difference in reactivity may be explained by steric factors: the pocket formed by the two hexamethylbenzene ligands is just big enough for pyrazole itself and pyrazole derivatives substituted only in 4-position, but it is too small for pyrazolato ligands which are substituted in 3- or 3- and 5-position.

2.2. Molecular structure of $[(\eta^6\text{-C}_6\text{Me}_6)_2\text{Ru}_2(\mu_2\text{-H})(\mu_2\text{-}\eta^1, \eta^1\text{-N}_2\text{C}_3\text{H}_3)_2]^+$ (**2**)

A single-crystal analysis has been performed on a single-crystal of the hexafluorophosphate salt of **2**. Suitable crystals have been obtained from a dichloromethane–hexane solution by the slow evaporation of the solvent. The molecular structure is depicted in Fig. 1. The hexafluorophosphate anion is not shown for reason of clarity. Important bond lengths and angles are presented in Table 2.

The cation is constructed of two $(\eta^6\text{-C}_6\text{Me}_6)\text{Ru}$ units, which are linked by two bridging $\mu_2\text{-}\eta^1, \eta^1$ -pyrazolato ligands. The bridging hydrido ligand could not be localized from an electron-density difference map, but its presence is clearly revealed by the ^1H NMR spectrum (Table 1). In addition, it can be deduced from the electron count and from the Ru–Ru distance of 3.090(2) Å, which is in agreement with a Ru_2H 3c–2e interaction or a Ru–Ru single bond. Due to the differ-

ence in size of the pyrazolato ligands and the hydrido ligand, the hexamethylbenzene rings are inclined with respect to each other by an angle of 58.8(4)°.

The geometry of the pyrazolato ligands as well as the Ru–N distances are as expected [15,25]. The distances between the C-3 and C-5 atoms of the pyrazolato ligands and the nearest methyl C-atoms of the hexamethylbenzene ligands [C(4)–C(17): 3.542(2), C(4)–C(18): 3.461(1), C(6)–C(30): 3.308(1) Å] as well as the distances in between the nearest methyl C-atoms of the inclined hexamethylbenzene ligands [C(13)–C(26): 3.845(2), C(14)–C(26): 3.803(2) Å] are quite close. This explains

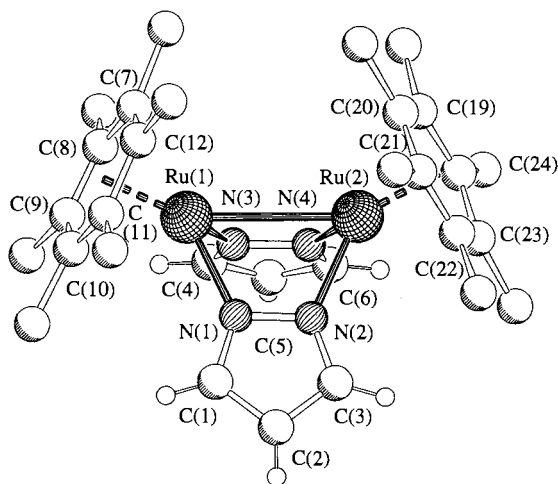


Fig. 1. Molecular structure of complex **2**. The alkyl protons have been omitted for clarity.

Table 2
Selected bond lengths [Å] and angles [°] for **2**

Interatomic distances	
Ru(1)–Ru(2)	3.090(2)
Ru(1)–N(1)	2.07(1)
Ru(2)–N(2)	2.10(1)
N(1)–N(2)	1.37(1)
Ru(1)–N(3)	2.09(1)
Ru(2)–N(4)	2.056(9)
N(3)–N(4)	1.37(1)
Ru(1)–C(7)	2.19(1)
Ru(1)–C(8)	2.20(2)
Ru(1)–C(9)	2.25(2)
Ru(1)–C(10)	2.24(1)
Ru(1)–C(11)	2.22(2)
Ru(1)–C(12)	2.24(1)
Ru(2)–C(19)	2.24(1)
Ru(2)–C(20)	2.23(2)
Ru(2)–C(21)	2.22(1)
Ru(2)–C(22)	2.23(1)
Ru(2)–C(23)	2.20(1)
Ru(2)–C(24)	2.21(1)
Bond angles	
N(1)–Ru(1)–Ru(2)	65.4(3)
N(2)–Ru(2)–Ru(1)	65.8(3)
N(3)–Ru(1)–Ru(2)	65.4(3)
N(4)–Ru(2)–Ru(1)	65.5(2)
Dihedral angles	
C(7)–C(12)/C(19)–C(24)	58.8(4)
N(1)–N(2)–C(1)–C(2)–C(3)/N(3)–N(4)–C(4)–C(5)–C(6)	86.9(4)

why 3- or 3,5-substituted pyrazoles do not react with **1** to give complexes analogous to **2**.

2.3. Reaction of $[(\eta^6\text{-C}_6\text{Me}_6)_2\text{Ru}_2(\mu_2\text{-H})_3]^+$ (**1**) with 1,2,4-triazole and 1,2,3-triazole

The reaction of $[(\eta^6\text{-C}_6\text{Me}_6)_2\text{Ru}_2(\mu_2\text{-H})_3]^+$ (**1**) with 1,2,4-triazole yields a disubstituted bistriazolato product, when it is carried out in an acidic medium (pH 3). After precipitation with KPF_6 and washing with a sodium hydroxide solution (pH 11), the complex $[(\eta^6\text{-C}_6\text{Me}_6)_2\text{Ru}_2(\mu_2\text{-H})(\mu_2\text{-}\eta^1, \eta^1\text{-N}_3\text{C}_2\text{H}_2)_2]^+$ (**4**) is obtained as the hexafluorophosphate salt (Scheme 2).

The ^1H NMR spectra of the hexafluorophosphate salt of **4** in acetone and of the sulfate salt in water confirm the presence of a bridging hydrido ligand and of two triazolato ligands containing four equivalent hydrogen atoms. The electrospray mass spectrum shows the unfragmented peak of cation **4** at m/z 665.

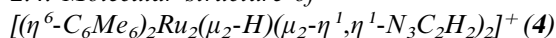
In complex **4**, both triazolato ligands are formally negative, the nitrogen atoms in 4-position have each a lone electron pair. Successive protonation of the ligands proved to be possible, giving the dicationic complex $[(\eta^6\text{-C}_6\text{Me}_6)_2\text{Ru}_2(\mu_2\text{-H})(\mu_2\text{-}\eta^1, \eta^1\text{-HN}_3\text{C}_2\text{H}_2)(\mu_2\text{-}\eta^1, \eta^1\text{-N}_3\text{C}_2\text{H}_2)]^{2+}$ (**5**) and the tricationic complex $[(\eta^6\text{-C}_6\text{Me}_6)_2\text{Ru}_2(\mu_2\text{-H})(\mu_2\text{-}\eta^1, \eta^1\text{-HN}_3\text{C}_2\text{H}_2)_2]^{3+}$ (**6**) (Scheme 3). It can be achieved by addition of HPF_6 to the acetone-solution of the hexafluorophosphate salt of **4** or by addition of H_2SO_4 to the aqueous solution of the sulfate salt. The protonation is reversible and can be inverted by addition of aqueous NaOH .

A ^1H NMR comparison of the cations **4**, **5**, and **6** (Table 1) shows a gradual downfield shift of all signals in going from **4** to **6**, being in line with the increase of the cationic charge from +1 to +3. The effect is very pronounced in the resonances of the triazolato ligands, which are the site of protonation. At room temperature (r.t.), the heterocyclic ligands of all three complexes give rise to one singlet, in water- d_2 as well as in acetone- d_6 . However, at -90°C , the spectrum of the monoprotonated complex **5** in acetone- d_6 exhibits two signals for the ligands. By this, a fast tautomeric exchange between the protonated triazole and the non-protonated triazolato ligand is proposed for complex **5**, a process which is frozen out at low temperatures (Scheme 3).

The reaction of **1** with 1,2,3-triazole also leads to disubstituted products in acidic media. Subsequent precipitation with KPF_6 gives a 1:1 mixture of the isomers of $[(\eta^6\text{-C}_6\text{Me}_6)_2\text{Ru}_2(\mu_2\text{-H})(\mu_2\text{-}\eta^1, \eta^1\text{-N}_3\text{C}_2\text{H}_2)_2]^+$, with the two triazolato ligands in a parallel (**7a**) or in an anti-parallel (**7b**) orientation (Scheme 2). While the ^1H NMR spectra of **7a** exhibit two different signals for the hexamethylbenzene ligands, those of **7b** reveal the equivalence of both arene ligands. These findings are in agreement with the structures presented in Scheme 2. The mixture of the isomers **7a** and **7b** is further characterized by the electrospray mass spectrum and microanalysis. In contrast to the bis-1,2,4-triazolato complex **4**, the bis-1,2,3-triazolato complexes **7a** and **7b** do not undergo protonation of the heterocyclic ligands in acidic solution.

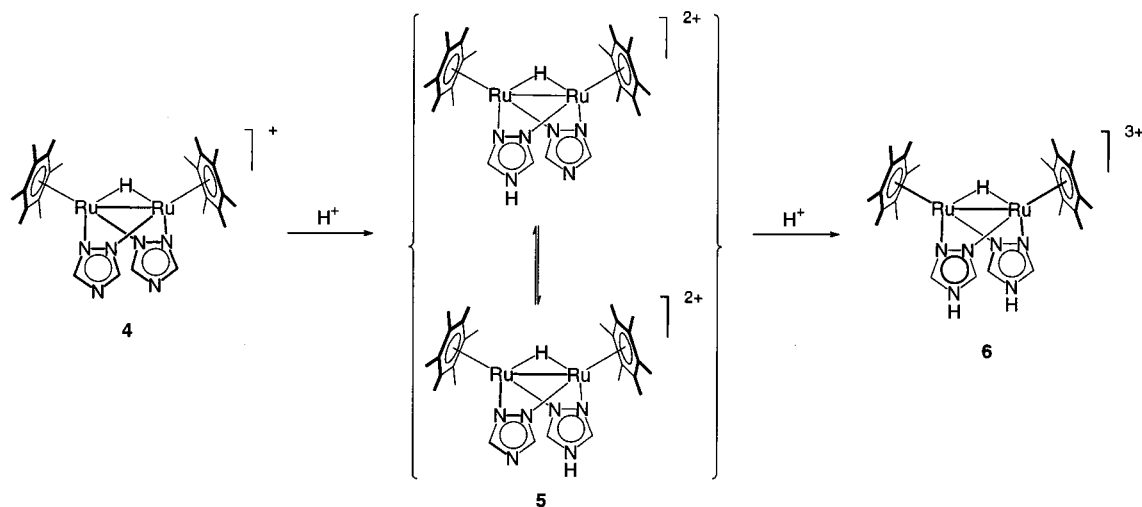
The reaction of **1** with 1,2,3-triazole also leads to disubstituted products in acidic media. Subsequent precipitation with KPF_6 gives a 1:1 mixture of the isomers of $[(\eta^6\text{-C}_6\text{Me}_6)_2\text{Ru}_2(\mu_2\text{-H})(\mu_2\text{-}\eta^1, \eta^1\text{-N}_3\text{C}_2\text{H}_2)_2]^+$, with the two triazolato ligands in a parallel (**7a**) or in an anti-parallel (**7b**) orientation (Scheme 2). While the ^1H NMR spectra of **7a** exhibit two different signals for the hexamethylbenzene ligands, those of **7b** reveal the equivalence of both arene ligands. These findings are in agreement with the structures presented in Scheme 2. The mixture of the isomers **7a** and **7b** is further characterized by the electrospray mass spectrum and microanalysis. In contrast to the bis-1,2,4-triazolato complex **4**, the bis-1,2,3-triazolato complexes **7a** and **7b** do not undergo protonation of the heterocyclic ligands in acidic solution.

2.4. Molecular structure of



Suitable crystals of the tosylate salt of **4** have been obtained by slow evaporation of the solvent from an aqueous solution at r.t. The crystal structure analysis reveals a unit cell containing two independent pairs of cations and anions. The parameters of both cationic molecules and both tosylate anions are very similar (Table 3). The arene rings of the tosylate anions are arranged side-by-side with one of the hexamethylbenzene rings of the respective cationic complex. The distinction between the two pairs per unit cell is based on the different orientations of the SO_3 -substituents in the two anions with regard to the orientation of the cations.

The molecular structure of one of the cations is depicted in Fig. 2. The two molecules of **4** present the

Scheme 3. Formation of complexes **5** and **6** by successive protonation of **4**.

same coordination and similar bond lengths and angles, as can be seen from Table 3. Cation **4** is constructed of two ($\eta^6\text{-C}_6\text{Me}_6$)Ru fragments, which are linked by two bridging $\mu_2\text{-}\eta^1,\eta^1$ -triazolato ligands and one bridging hydrido ligand. The analogy in the constitution of the 1,2,4-triazolato complex **4** to that of the pyrazolato complex **2** is reflected in the similarity of the structural parameters (cf. Tables 2 and 3). The Ru–Ru distance of 3.102(1) (molecule 1) and 3.098(1) Å (molecule 2) is as to be expected for a hydrido-bridged Ru–Ru $3c\text{--}2e$ interaction, i.e. a formal Ru–Ru single bond, and is almost identical with that in **2** [3.090(2) Å]. The inclination of the two hexamethylbenzene rings of 61.9(5) and 61.0(5)°, which is due to the different steric requirements of the bridging ligands, and the angles between the coordinated heterocyclic ligands of 80.4(6) and 83.6(6)° compare well to the parameters in **2** [58.8(4) and 86.9(4)°, respectively].

The unit cell of **4** contains, in addition to the two pairs of cations and anions, nine water molecules—four of which are hydrogen-bonded to the non-coordinating nitrogen atom of the triazolato ligands, while the two tosylate anions are hydrogen-bonded to two other water molecules each, the ninth H₂O molecule being hydrogen-bonded to one of these water molecules. The presence of a hydrogen-bonded water molecule at the non-coordinating N atom of each triazolato ligand indicates the possibility to protonate the coordinated triazoles. This protonation does indeed take place in acidic media leading to complexes **5** and **6**, successively.

2.5. Molecular structure of $[(\eta^6\text{-C}_6\text{Me}_6)_2\text{Ru}_2(\mu_2\text{-H})_3]^+$ (**1**)

The title complex $[(\eta^6\text{-C}_6\text{Me}_6)_2\text{Ru}_2(\mu_2\text{-H})_3]^+$ (**1**) is known since 1982 [11], but its structure has never been reported. We therefore undertook to grow crystals of a

salt of **1** suitable for a single-crystal X-ray structure analysis. Suitable crystals have been obtained as follows: ethanol was carefully added to the red aqueous solution of the sulfate salt of **1** to give a top layer of colorless ethanol. Subsequently, an ethanolic solution of NH_4PF_6 was carefully added to the ethanol layer. Diffusion gave small crystals of the hexafluorophosphate salt of **1** after several days.

The molecular structure of **1** is depicted in Fig. 3. The hexafluorophosphate anion is omitted for clarity. Important bond lengths and angles are given in Table 4. The molecule consists of two ($\eta^6\text{-C}_6\text{Me}_6$)Ru units, linked by three bridging hydrido ligands. It possesses a crystallographic mirror plane bisecting both ruthenium atoms and the hexamethylbenzene ligands. The hydrido ligands could be located from an electron-density difference map, one being positioned on the mirror plane.

The very short Ru–Ru distance of 2.4681(4) Å accounts for the formal metal–metal triple-bond, which has to be interpreted as a $5c\text{--}6e$ interaction of the two ruthenium atoms and the three hydrogen atoms. It compares well to that of 2.474 Å in the homologous mesitylene–osmium complex [26] and even in the same range as that of 2.4630 Å in the quadruply hydrido-bridged complex $[(\eta^5\text{-C}_5\text{Me}_5)_2\text{Ru}_2(\mu_2\text{-H})_4]$ [27]. As to be expected, the hexamethylbenzene rings are nearly parallel, with a dihedral angle of only 1.3(7)°.

3. Experimental section

3.1. General

All manipulations were carried out under nitrogen atmosphere, using standard Schlenk techniques. The bidistilled water was degassed and saturated with inert gas prior to use. The organic solvents were refluxed

Table 3
Selected bond lengths [Å] and angles [°] for **4**

Molecule 1		Molecule 2	
Interatomic distances		Interatomic distances	
Ru(1)–Ru(2)	3.102(1)	Ru(3)–Ru(4)	3.098(1)
Ru(1)–H(1Ru)	2.0(1)	Ru(3)–H(2Ru)	1.67(8)
Ru(2)–H(1Ru)	1.9(1)	Ru(4)–H(2Ru)	1.72(8)
Ru(1)–N(1)	2.08(1)	Ru(3)–N(7)	2.11(1)
Ru(2)–N(2)	2.05(1)	Ru(4)–N(8)	2.06(1)
N(1)–N(2)	1.38(2)	N(7)–N(8)	1.35(2)
Ru(1)–N(4)	2.12(1)	Ru(3)–N(10)	2.13(1)
Ru(2)–N(5)	2.08(1)	Ru(4)–N(11)	2.09(1)
N(4)–N(5)	1.38(2)	N(10)–N(11)	1.37(2)
Ru(1)–C(5)	2.27(5)	Ru(3)–C(33)	2.20(2)
Ru(1)–C(6)	2.20(2)	Ru(3)–C(34)	2.24(2)
Ru(1)–C(7)	2.20(2)	Ru(3)–C(35)	2.21(2)
Ru(1)–C(8)	2.18(2)	Ru(3)–C(36)	2.20(2)
Ru(1)–C(9)	2.20(1)	Ru(3)–C(37)	2.18(2)
Ru(1)–C(10)	2.24(2)	Ru(3)–C(38)	2.20(2)
Ru(2)–C(17)	2.19(5)	Ru(4)–C(45)	2.20(2)
Ru(2)–C(18)	2.21(2)	Ru(4)–C(46)	2.25(2)
Ru(2)–C(19)	2.21(2)	Ru(4)–C(47)	2.20(2)
Ru(2)–C(20)	2.19(2)	Ru(4)–C(48)	2.23(2)
Ru(2)–C(21)	2.25(2)	Ru(4)–C(49)	2.21(2)
Ru(2)–C(22)	2.23(2)	Ru(4)–C(50)	2.18(2)
Hydrogen bonds		Hydrogen bonds	
N(3)...O(1W)	2.86(2)	N(9)...O(3W)	2.84(2)
N(6)...O(2W)	2.90(2)	N(12)...O(4W)	2.88(2)
Bond angles		Bond angles	
N(1)–Ru(1)–Ru(2)	65.4(4)	N(7)–Ru(3)–Ru(4)	64.6(3)
N(2)–Ru(2)–Ru(1)	65.2(4)	N(8)–Ru(4)–Ru(3)	65.6(3)
N(4)–Ru(1)–Ru(2)	65.4(4)	N(10)–Ru(3)–Ru(4)	65.7(3)
N(5)–Ru(2)–Ru(1)	66.1(3)	N(11)–Ru(4)–Ru(3)	65.9(3)
Dihedral angles		Dihedral angles	
C(5)–C(10)/C(17)–C(22)	61.9(5)	C(33)–C(38)/C(45)–C(50)	61.0(5)
N(1)–N(2)–C(1)–N(3)–C(2)/N(4)–N(5)–C(3)–N(6)–C(4)	80.4(6)	N(7)–N(8)–C(29)–N(9)–C(30)/N(10)–N(11)–C(31)–N(12)–C(32)	83.6(6)

over appropriate desiccants [28], distilled, and saturated with inert gas. The NMR spectra were recorded on a Varian Gemini 200 BB instrument, the treatment was performed using a SUN Varian station. The NMR spectra of complex **7** (isomer mixture) were recorded on a Bruker AMX-400 instrument. The IR spectra were recorded on a Perkin-Elmer FTIR 1720 X spectrophotometer (4000–400 cm⁻¹) as KBr pellets. Microanalytical data were obtained by the Mikroelementar-analytisches Laboratorium ETH Zürich. The FAB mass spectrum of **4** was measured by Prof. Titus A. Jenny, Institut de Chimie Organique, Université de Fribourg, Switzerland. Electrospray mass spectra of the hexafluorophosphate salts of complexes **1** and **3–7** were obtained in positive-ion mode with a LCQ Finnigan mass spectrometer using acetone as the mobile phase. The starting material ($\eta^6\text{-C}_6\text{Me}_6$)₂Ru₂Cl₄ was synthesized according to the literature procedure [29]. All other reagents were commercially available and were used without further purification.

3.2. Preparation of $[(\eta^6\text{-C}_6\text{Me}_6)_2\text{Ru}_2(\mu_2\text{-H})_3]^+$ (**1**)

A mixture of ($\eta^6\text{-C}_6\text{Me}_6$)₂Ru₂Cl₄ (100 mg, 0.150 mmol) and Ag₂SO₄ (94 mg, 0.300 mmol) in water (20 ml) is stirred in a Schlenk tube for 1 h in the dark (aluminum foil). During this period the mixture is treated several times with ultrasound (ca. 1 min), until all orange solids are dissolved. After filtration of the silver chloride that precipitates, the yellow solution containing $[(\eta^6\text{-C}_6\text{Me}_6)\text{Ru}(\text{H}_2\text{O})_3]^{2+}$ is employed in situ in order to prepare $[(\eta^6\text{-C}_6\text{Me}_6)_2\text{Ru}_2(\mu\text{-H})_3]^+$ (**1**). For this, an aqueous solution of NaBH₄ (20 mg, 0.529 mmol, 15 ml H₂O) is added dropwise to the solution of $[(\eta^6\text{-C}_6\text{Me}_6)\text{Ru}(\text{H}_2\text{O})_3]^{2+}$ (0.300 mmol, 20 ml H₂O). The color turns dark-green upon addition of the first drops, but eventually the solution becomes dark red. It is filtered in order to remove a fine black precipitate which has formed during the reaction. This aqueous solution of $[(\eta^6\text{-C}_6\text{Me}_6)_2\text{Ru}_2(\mu\text{-H})_3]^+$ is used in situ

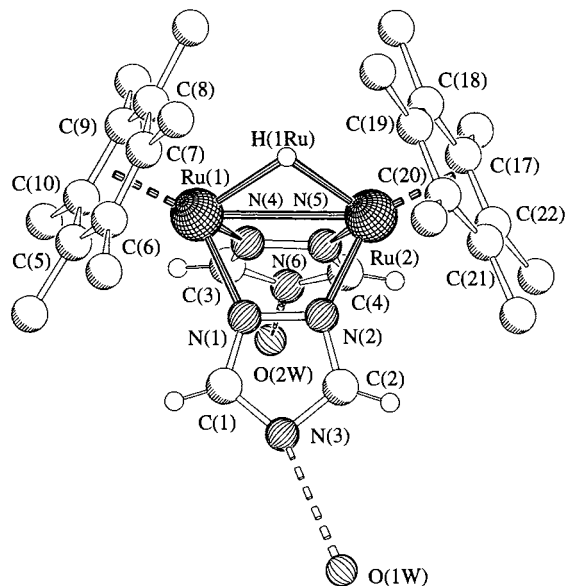


Fig. 2. Molecular structure of complex **4**. The alkyl protons have been omitted for clarity.

without further work-up. For this reason, the molar quantities of **1**—given in parentheses—as well as the yields of the new complexes are based on the quantity of $(\eta^6\text{-C}_6\text{Me}_6)_2\text{Ru}_2\text{Cl}_4$ employed. For the characterization compare Ref. [9]. MS (m/z): 531, cation **1**.

3.3. Preparation of $[(\eta^6\text{-C}_6\text{Me}_6)_2\text{Ru}_2(\mu_2\text{-H})(\mu_2\text{-}\eta^1, \eta^1\text{-N}_2\text{C}_3\text{H}_3)_2]^+$ (**2**)

Pyrazole (15 mg, 0.22 mmol) is added to an aqueous solution of $[(\eta^6\text{-C}_6\text{Me}_6)_2\text{Ru}_2(\mu\text{-H})_3]_2[\text{SO}_4]$ (cation **1**) (0.038 mmol, 30 ml H_2O , pH 3). The solution is heated to 100°C in a closed pressure Schlenk tube for 3 h. The reaction also proceeds at r.t. within 1 day. After filtration, the product is precipitated by addition of an excess of NH_4PF_6 . The mixture is then filtrated and the

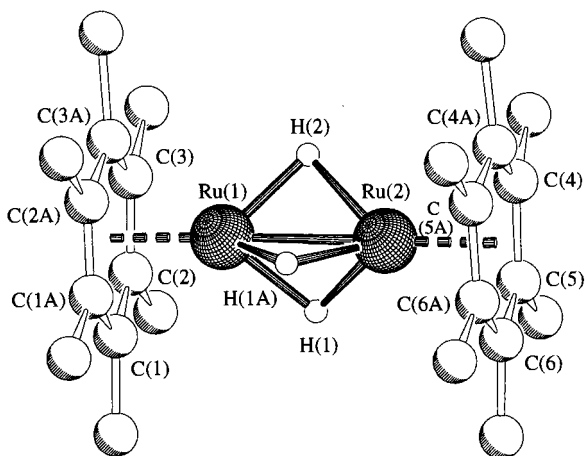


Fig. 3. Molecular structure of complex **1**. The alkyl protons have been omitted for clarity.

Table 4
Selected bond lengths [Å] and angles [°] for **1**

Interatomic distances	
Ru(1)–Ru(2)	2.4681(4)
Ru(1)–C(1)	2.23(1)
Ru(1)–C(2)	2.20(1)
Ru(1)–C(3)	2.18(1)
Ru(2)–C(4)	2.18(1)
Ru(2)–C(5)	2.23(1)
Ru(2)–C(6)	2.24(1)
Ru(1)–H(1)	1.76(4)
Ru(2)–H(1)	1.68(4)
Ru(1)–H(2)	1.74(4)
Ru(2)–H(2)	1.87(4)
Dihedral angles	
C(1)–C(2)–C(3)/C(4)–C(5)–C(6)	1.3(7)

precipitate washed with water (2×5 ml). Drying in vacuo gives $[(\eta^6\text{-C}_6\text{Me}_6)_2\text{Ru}_2(\mu_2\text{-H})(\mu_2\text{-}\eta^1, \eta^1\text{-N}_2\text{C}_3\text{H}_3)_2][\text{PF}_6]$ (cation **2**) (50 mg, 0.06 mmol, 82%) as a red powder. **2** [PF_6]. Anal. Calcd. for $\text{C}_{30}\text{H}_{43}\text{F}_6\text{N}_4\text{P}_1\text{Ru}_2$: C, 44.66; H, 5.37; N, 6.94. Found: C, 44.34; H, 5.64; N, 7.05. ^{13}C NMR (δ , acetone- d_6): 16.87 ($\text{C}_6(\text{CH}_3)_6$), 94.62 ($\text{C}_6(\text{CH}_3)_6$), 105.56 (C4), 136.95, 137.02 (C₃, C5). MS (m/z): 663, cation **2**.

3.4. Preparation of $[(\eta^6\text{-C}_6\text{Me}_6)_2\text{Ru}_2(\mu_2\text{-H})(\mu_2\text{-}\eta^1, \eta^1\text{-N}_2\text{C}_3\text{H}_2\text{CH}_3)_2]^+$ (**3**)

4-Methylpyrazole (20 ml, 0.24 mmol) is added to an aqueous solution of $[(\eta^6\text{-C}_6\text{Me}_6)_2\text{Ru}_2(\mu\text{-H})_3]_2[\text{SO}_4]$ (cation **1**) (0.025 mmol, 20 ml H_2O , pH 3), and the solution is stirred for 3 days at r.t. Precipitation with an excess of NH_4PF_6 , filtration, washing with water (2×5 ml), and drying in vacuo gives $[(\eta^6\text{-C}_6\text{Me}_6)_2\text{Ru}_2(\mu_2\text{-H})(\mu_2\text{-}\eta^1, \eta^1\text{-N}_2\text{C}_3\text{H}_2\text{CH}_3)_2][\text{PF}_6]$ (cation **3**) (38 mg, 0.045 mmol, 90%) as a red powder. **3** [PF_6]. Anal. Calcd. for $\text{C}_{32}\text{H}_{47}\text{F}_6\text{N}_4\text{P}_1\text{Ru}_2 \cdot 0.5 \text{H}_2\text{O}$: C, 45.55; H, 5.73; N, 6.64. Found: C, 45.47; H, 5.82; N, 6.80. ^{13}C NMR (δ , acetone- d_6): 8.54 (4-Mepz), 16.87 ($\text{C}_6(\text{CH}_3)_6$), 94.42 ($\text{C}_6(\text{CH}_3)_6$), 115.50 (C4), 136.45 (C3/C5). MS (m/z): 691, cation **3**.

3.5. Preparation of $[(\eta^6\text{-C}_6\text{Me}_6)_2\text{Ru}_2(\mu_2\text{-H})(\mu_2\text{-}\eta^1, \eta^1\text{-N}_3\text{C}_2\text{H}_2)_2]^+$ (**4**)

1,2,4-Triazole (14 mg, 0.20 mmol) is added to an aqueous solution of $[(\eta^6\text{-C}_6\text{Me}_6)_2\text{Ru}_2(\mu\text{-H})_3]_2[\text{SO}_4]$ (cation **1**) (0.049 mmol, 15 ml H_2O , pH 3). After 1 day of stirring at r.t., the solution is reduced in volume to 8 ml. An excess of KPF_6 is added in order to precipitate a red powder, which is then centrifuged. Washing with an aqueous NaOH -solution (pH 11, 2×3 ml) and drying in vacuo gives $[(\eta^6\text{-C}_6\text{Me}_6)_2\text{Ru}_2(\mu_2\text{-H})(\mu_2\text{-}\eta^1, \eta^1\text{-N}_3\text{C}_2\text{H}_2)_2][\text{PF}_6]$ (cation **4**) (24 mg, 0.030 mmol, 66%) as a dark red powder. **4** [PF_6]. Anal. Calcd. for

Table 5
Crystallographic and selected experimental data for **1**, **2** and **4**

Compound	$[(\eta^6\text{-C}_6\text{Me}_6)_2\text{-Ru}_2(\mu_2\text{-H})_3][\text{PF}_6]$ (cation 1)	$[(\eta^6\text{-C}_6\text{Me}_6)_2\text{Ru}_2(\mu_2\text{-H})\text{-}(\mu_2\text{-}\eta^1, \eta^1\text{-N}_3\text{C}_2\text{H}_2)_2][\text{PF}_6]$ (cation 2)	$[(\eta^6\text{-C}_6\text{Me}_6)_2\text{Ru}_2(\mu_2\text{-H})\text{-}(\mu_2\text{-}\eta^1, \eta^1\text{-N}_3\text{C}_2\text{H}_2)_2][\text{C}_7\text{H}_7\text{SO}_3]$ (cation 4)
Formula	$\text{C}_{24}\text{H}_{39}\text{F}_6\text{PRu}_2$	$\text{C}_{30}\text{H}_{43}\text{F}_6\text{N}_4\text{PRu}_2$	$\text{C}_{35}\text{H}_{48}\text{N}_6\text{O}_3\text{Ru}_2\text{S} \cdot 4.5 \text{H}_2\text{O}$
Crystal shape	Block	Block	Plate
Crystal color	Violet	Dark brown to black	Red
Crystal size (mm)	$0.15 \times 0.15 \times 0.15$	$0.50 \times 0.34 \times 0.19$	$0.57 \times 0.38 \times 0.08$
Crystal system	Monoclinic	Monoclinic	Triclinic
<i>M</i>	674.66	806.79	916.07
Space group	<i>Am</i>	<i>P2</i> ₁ / <i>n</i>	<i>P1</i>
<i>a</i> (Å)	10.0367(10)	13.009(6)	8.7659(7)
<i>b</i> (Å)	12.4540(8)	16.860(8)	14.7894(12)
<i>c</i> (Å)	10.8468(10)	14.642(7)	17.506(2)
α (°)	90	90	67.058(6)
β (°)	99.190(12)	100.51(3)	77.422(9)
γ (°)	90	90	73.228(10)
<i>V</i> (Å ³)	1338.4(2)	3158(3)	1986.8(3)
<i>Z</i>	2	4	2
<i>D</i> _{calc.} (g cm ⁻³)	1.674	1.697	1.531
μ (Mo–K α) (mm ⁻¹)	1.240	1.070	0.867
<i>F</i> (000)	680	1632	946
θ Scan range (°)	2.06–25.88	2.00–25.00	2.31–25.50
<i>T</i> (K)	223(2)	223(2)	293(2)
<i>N</i> Standards	—	2	2
Intensity variation	—	<2%	<2%
Reflections measured	5258	5562	7392
Independent reflections	2470	5562	7392
Reflections observed [<i>I</i> > 2 σ (<i>I</i>)]	2207	4163	6322
Final <i>R</i> indices [<i>I</i> > 2 σ (<i>I</i>)] ^a	$R_1 = 0.0236$, $wR_2 = 0.0567$	$R_1 = 0.0874$, $wR_2 = 0.2175$	$R_1 = 0.0477$, $wR_2 = 0.1069$
<i>R</i> indices (all data) ^a	$R_1 = 0.0275$, $wR_2 = 0.0576$	$R_1 = 0.1240$, $wR_2 = 0.2952$	$R_1 = 0.0624$, $wR_2 = 0.1243$
Goodness of fit	1.003	1.111	1.152
Maximum Δ (σ)	0.073	–0.002	–1.310
Residual density: maximum, minimum $\Delta\rho$ (e Å ⁻³)	0.723, –0.831	1.181, –1.823	0.887, –0.975

$${}^a R_1 = \frac{\sum |F_o| - |F_c|}{\sum |F_o|}, \quad wR_2 = \left[\frac{\sum w(F_o^2 - F_c^2)^2}{\sum wF_o^4} \right]^{1/2}.$$

$\text{C}_{28}\text{H}_{41}\text{F}_6\text{N}_6\text{P}_1\text{Ru}_2 \cdot 1.5 \text{H}_2\text{O}$: C, 40.24; H, 5.31; N, 10.06. Found: C, 40.35; H, 5.01; N, 10.09. MS (*m/z*): 665, cation **4**.

3.6. Preparation of $[(\eta^6\text{-C}_6\text{Me}_6)_2\text{Ru}_2(\mu_2\text{-H})(\mu_2\text{-}\eta^1, \eta^1\text{-HN}_3\text{C}_2\text{H}_2)(\mu_2\text{-}\eta^1, \eta^1\text{-N}_3\text{C}_2\text{H}_2)]^{2+}$ (**5**)

The synthesis of **5** follows that of **4** until the precipitation with KPF_6 and the centrifugation of the red powder. Washing with an aqueous HPF_6 -solution (pH 2, 2×3 ml) and drying in vacuo gives $[(\eta^6\text{-C}_6\text{Me}_6)_2\text{Ru}_2(\mu_2\text{-H})(\mu_2\text{-}\eta^1, \eta^1\text{-HN}_3\text{C}_2\text{H}_2)(\mu_2\text{-}\eta^1, \eta^1\text{-N}_3\text{C}_2\text{H}_2)][\text{PF}_6]_2$ (cation **5**) (29 mg, 0.030 mmol, 66%) as a red powder. **5** $[\text{PF}_6]_2$. Anal. Calcd. for $\text{C}_{28}\text{H}_{42}\text{F}_{12}\text{N}_6\text{P}_2\text{Ru}_2$: C, 35.22; H, 4.43; N, 8.80. Found: C, 34.91; H, 4.51; N, 9.09. MS (*m/z*): 665, cation **4** (i.e. deprotonation).

3.7. Preparation of $[(\eta^6\text{-C}_6\text{Me}_6)_2\text{Ru}_2(\mu_2\text{-H})(\mu_2\text{-}\eta^1, \eta^1\text{-HN}_3\text{C}_2\text{H}_2)]^{3+}$ (**6**)

The synthesis of **6** also follows that of **4** until the precipitation with KPF_6 and the centrifugation of the red powder. Washing with an aqueous HPF_6 -solution (pH 0, 2×3 ml) and drying in vacuo gives $[(\eta^6\text{-C}_6\text{Me}_6)_2\text{Ru}_2(\mu_2\text{-H})(\mu_2\text{-}\eta^1, \eta^1\text{-HN}_3\text{C}_2\text{H}_2)_2][\text{PF}_6]_3$ (cation **6**) (28 mg, 0.026 mmol, 58%) as an orange powder. **6** $[\text{PF}_6]_3$. Anal. Calcd. for $\text{C}_{28}\text{H}_{43}\text{F}_{18}\text{N}_6\text{P}_3\text{Ru}_2$: C, 30.55; H, 3.94; N, 7.64. Found: C, 30.64; H, 4.14; N, 7.83. MS (*m/z*): 665, cation **4** (i.e. deprotonation).

3.8. Preparation of $[(\eta^6\text{-C}_6\text{Me}_6)_2\text{Ru}_2(\mu_2\text{-H})(\mu_2\text{-}\eta^1, \eta^1\text{-N}_3\text{C}_2\text{H}_2)]^+$ (**7**)

1H-1,2,3-Triazole (30 μl , 36 mg, 0.52 mmol) is added to an aqueous solution of $[(\eta^6\text{-C}_6\text{Me}_6)_2\text{Ru}_2(\mu_2\text{-H})(\mu_2\text{-}\eta^1, \eta^1\text{-N}_3\text{C}_2\text{H}_2)]^+$ (**7**).

H)₃]₂[SO₄] (cation **1**) (0.049 mmol, 15 ml H₂O, pH 3). After two days of stirring at r.t., or also after 3 h at 95°C in a pressure Schlenk tube, the product is precipitated by addition of an excess of KPF₆, and then centrifuged. Washing with water (2 × 3 ml) and drying in vacuo gives [(η⁶-C₆Me₆)₂Ru₂(μ₂-H)(μ₂-η¹,η¹-N₃C₂H₂)₂][PF₆] (cation **7**) (31 mg, 0.038 mmol, 78%) as a red powder. **7** [PF₆]. Anal. Calcd. for C₂₈H₄₁F₆N₆P₁Ru₂: C, 41.58; H, 5.11; N, 10.39. Found: C, 41.50; H, 4.93; N, 10.53. MS (*m/z*): 665, cation **7**.

3.9. X-ray structure determination of complexes **1**, **2** and **4**

For **2** and **4**, the X-ray data were recorded using a Stoe-Siemens AED2 4-circle diffractometer (Mo-K_α graphite monochromated radiation, λ = 0.71073 Å; ω/2θ scans). Two standard reflections were measured every hour and indicated only a small intensity variation (ca. 2%) for both complexes. For **1**, data collection was performed with a Stoe Imaging Plate Diffractometer System (Stoe and Cie, 1995) equipped with a one-circle φ goniometer and a graphite-monochromator, using Mo-K_α radiation (λ = 0.71073 Å); 200 exposures (3 min per exposure) were obtained at an image plate distance of 70 mm with 0 < φ < 200° and with the crystal oscillating through 1° in φ, resolution D_{min}-D_{max} 12.45-0.81 Å. Table 5 summarizes the crystallographic and selected experimental data for **1**, **2**, and **4**.

The structures were solved by Direct Methods using the program SHELXS 86 [30] and refined by full-matrix least-squares on F² using the program SHELXL 93 [31]. The figures were drawn with SCHAKAL [32]. Important bond lengths and angles are given in Table 2 for **2**, in Table 3 for **4**, and in Table 4 for **1**. The hydrido ligands were located from difference maps for **1** and **4**. They were fully refined for **4**, and refined with the ruthenium-hydride bonds being constrained to a distance of 1.8 Å, using a high estimated S.D. of 0.05 Å, for **1**. The methyl hydrogens of the hexamethylbenzene ligands in all three structures and the aromatic hydrogen atoms of the heterocyclic ligands in **2** and **4** were included in calculated positions and refined as riding atoms using the SHELXL 93 default parameters.

Acknowledgements

We thank the Swiss National Science Foundation for financial support of this work and the Johnson Matthey Research Center for a generous loan of ruthenium(III) chloride hydrate.

References

- [1] M. Barton, J.D. Atwood, J. Coord. Chem. 24 (1991) 43.
- [2] (a) W.A. Hermann, C.W. Kohlpaintner, Angew. Chem. Int. Ed. Engl. 32 (1993) 1524. (b) W.A. Hermann, C.W. Kohlpaintner, Angew. Chem. 105 (1993) 1588.
- [3] U. Bodensieck, A. Meister, G. Rheinwald, H. Stoeckli-Evans, G. Süss-Fink, Chimia 47 (1993) 189.
- [4] G. Meister, G. Rheinwald, H. Stoeckli-Evans, G. Süss-Fink, J. Chem. Soc., Dalton Trans. (1994) 3215.
- [5] F. von Gyldenfeldt, D. Marton, G. Tagliavini, Organometallics 13 (1994) 906.
- [6] U. Koelle, Coord. Chem. Rev. 135/136 (1994) 623.
- [7] G. Süss-Fink, A. Meister, G. Meister, Coord. Chem. Rev. 143 (1995) 97.
- [8] G. Meister, G. Rheinwald, H. Stoeckli-Evans, G. Süss-Fink, J. Organomet. Chem. 496 (1995) 197.
- [9] M. Jahncke, G. Meister, G. Rheinwald, H. Stoeckli-Evans, G. Süss-Fink, Organometallics 16 (1997) 1137.
- [10] M. Jahncke, A. Neels, H. Stoeckli-Evans, G. Süss-Fink, J. Organomet. Chem. (in print).
- [11] M.A. Bennett, J.P. Ennett, K.I. Gell, J. Organomet. Chem. 233 (1982) C17.
- [12] M.A. Bennett, J.P. Ennett, Inorg. Chim. Acta 198–200 (1992) 583.
- [13] A.P. Sadimenko, S.S. Basson, Coord. Chem. Rev. 147 (1996) 247.
- [14] C.W. Eigenbrot, K.N. Raymond, Inorg. Chem. 21 (1982) 2653.
- [15] W.S. Sheldrick, H.-S. Hagen-Eckhard, J. Organomet. Chem. 410 (1991) 73.
- [16] D. Carmona, F.J. Lahoz, R. Atencio, et al., Inorg. Chem. 35 (1996) 2549.
- [17] D. Carmona, A. Mendoza, J. Ferrer, F.J. Lahoz, L.A. Oro, J. Organomet. Chem. 431 (1992) 87.
- [18] L.A. Oro, M.P. Garcia, D. Carmona, C. Foces-Foces, F.H. Cano, Inorg. Chim. Acta 96 (1985) 21.
- [19] A. Michalowicz, J. Moscovici, B. Ducourant, D. Cracco, O. Kahn, Chem. Mater. 7 (1995) 1833.
- [20] W. Vreugdenhill, J.G. Haasnoot, J. Reedijk, J.S. Wood, Inorg. Chim. Acta 167 (1990) 109.
- [21] G. Vos, R.A.G. de Graaff, J.G. Haasnoot, A.M. van der Kraan, P. de Vaal, J. Reedijk, Inorg. Chem. 23 (1984) 2905.
- [22] G.A. van Albada, R.A.G. de Graaff, J.G. Haasnoot, J. Reedijk, Inorg. Chem. 23 (1984) 1404.
- [23] J. Kroeber, I. Bkouche-Waksman, C. Pascard, M. Thomann, O. Kahn, Inorg. Chim. Acta 230 (1995) 159.
- [24] M. Stebler-Röthlisberger, A. Ludi, Polyhedron 5 (1986) 1217.
- [25] A.G. Orpen, L. Brammer, F.H. Allen, O. Kennard, D.G. Watson, R. Taylor, J. Chem. Soc., Dalton Trans. (1989) S1.
- [26] M. Schulz, S. Stahl, H. Werner, J. Organomet. Chem. 394 (1990) 469.
- [27] H. Suzuki, H. Omori, D.H. Lee, et al., Organometallics 13 (1994) 1129.
- [28] D.D. Perrin, W.L.F. Armarego, Purifications of Laboratory Chemicals, 3rd ed, Pergamon Press, Oxford, UK, 1988.
- [29] M.A. Bennett, T.-N. Huang, T.W. Matheson, A.K. Smith, Inorg. Synth. 21 (1982) 74.
- [30] SHELXS 86, G.M. Sheldrick, Acta Crystallogr., Sect. A 46 (1990) 467.
- [31] SHELXL 93, G.M. Sheldrick, A program for crystal structure refinement, University of Göttingen, Göttingen, Germany, 1993.
- [32] SCHAKAL 92/V256, E. Keller: A Fortran program for the graphical representation of molecular and crystallographic models, University of Freiburg, Germany, 1992.